ORIGINAL ARTICLE

Novel flourescent spiroborate esters: potential therapeutic agents in in vitro cancer models

S. Anjana[1] · Josna Joseph[2] · Jeena John[3] · S. Balachandran[3] · T. R. Santhosh Kumar[4] · Annie Abraham[2]

Abstract

The current treatment system in cancer therapy, which includes chemotherapy/radiotherapy is expensive and often deleterious to surrounding healthy tissue. Presently, several medicinal plants and their constituents are in use to manage the development and progression of these diseases.They have been found effective, safe, and less expensive. In the present study, we are proposing the utility of a new class of curcumin derivative, Rubrocurcumin, the spiroborate ester of curcumin with boric acid and oxalic acid (1:1:1), which have enhanced biostability for therapeutic applications. In vitro cytocompatibility of this drug complex was analysed using MTT assay, neutral red assay, lactate dehydrogenase assay in 3T3L1 adipocytes. Anti tumour activity of this drug complex on MCF7 and A431 human cancer cell line was studied by morphological analysis using phase contrast microscopy, Hoechst staining and cell cycle analysis by FACS. To explore the chemotherapeutic effect, the cytotoxic effect of this compound was also carried out. Rubrocurcumin is more biostable than natural curcumin in physiological medium. Our results prove that this curcumin derivative drug complex possess more efficacy and anti-cancer activity compared with curcumin. The findings out of this study suggests this novel compound as potential candidate for site targeted drug delivery.

Keywords Curcumin · Skin cancer · Drug delivery · Natural product · Anti-cancer agent

Introduction

Skin cancer cases are widely being reported worldwide. It is estimated that more than 9500 people in the U.S. are diagnosed with skin cancer every day [1], whereas fewer incidence are reported in tropical nations like India and Africa. The major types of skin cancer are basal cell carcinoma, squamous cell carcinoma and melanoma. The current treatment regimen including surgery, radiotherapy and chemotherapy cream are effective in managing the situation, but with their own side effects. Also, skin cancer can at times

result due to inflammation [2] necessitating the search for a drug with anti-inflammatory property with low side effects.

Though the cancer of colon, lung, prostate and breast occur commonly around the world, there are only ten times lower incident reports in India [3]. This may be attributed to the regular consumption of the flavonoid curcumin containing turmeric, which is a prominent spice in Indian cuisine. Curcumin plays an important role in slowing down the progression of skin cancer and it has curative properties. It is hypothesized that curcumin has growth-inhibitory effects through the TOR pathway [4] and chemopreventive potential in skin sarcoma where local application could bypass bioavailability problems. It has also been reported that curcumin had been used in the form of a skin ointment for the treatment of basal cell carcinoma [5].

Of all types of skin cancers, melanoma is the most fatal. Curcumin arise as a potent natural drug,which is powerful enough to arrest the growth of cancer cells without being cytotoxic to normal cells [6]. Sometimes, melanoma can become resistant to chemotherapy and in such cases turmeric offers greater application. This is because curcumin is able to trigger the clean up of dysfunctional cellular components

✉ Annie Abraham
  annieab2013@gmail.com

1 Department of Biotechnology, University of Kerala, Thiruvananthapuram, Kerala, India

2 Department of Biochemistry, University of Kerala, Thiruvananthapuram, Kerala, India

3 Department of Chemistry, MG College, Thiruvananthapuram, Kerala, India

4 Rajiv Gandhi Centre for Biotechnology, Thiruvananthapuram, Kerala, India

\ Springer

[7]. Curcumin could prevent skin cancer and it protects the skin by eliminating free radicals and reducing inflammation through inhibition of factors involved in tumour formation. Besides, it also protects the skin from various kinds of oxidative stress [8]. This is attributed to triggering phase II detoxification enzymes which have prominent role in detoxification reactions.

Low bioavailability of curcumin is an impediment to its transition to clinical trials. Application of curcumin containing cream for skin cancer treatment, solves this problem since curcumin is known to slow down the progress of the skin cancer. In spite of its promising chemotherapeutic activity, pre-clinical and clinical studies reveal curcumin's limited therapeutic application, due to its instability in physiological condition, poor solubility and higher metabolic activity [9]. One of the highly promising approaches to overcome this instability and bioavailability issue is to convert curcumin to its metal complex and many such curcumin complexes are reported in literature [10]. Spiroborate esters of curcumin are of good choice since they are more stable than curcumin in solid state and in water mediated condition [11, 12]. More over, the components of these complexes i.e., curcumin, boric acid and dicarboxylic acid/hydroxy acids are in use in many ayurvedic and other medical formulations [13] and are reported to be non toxic. Majority of skin protection ointments contain oxalic acid and boric acid, which are well known antibacterial agents. Reports show that combination of oxalic acid, boric acid and curcumin could result in the formation of another compound, rubrocurmin which is highly stable in oil medium [10].

In the present study, a series of mixed spiroborate esters of curcumin were subjected to preliminary analysis against different cancer cells. Four spiroborate esters of curcumin formed by the condensation of oxalic acid, malonic acid, salicylic acid and citric acid with curcumin and boric acid (Fig. 1) were used for the primary analysis against cancer cells. Among these, the oxalic acid complex, Rubrocurcumin is a suggestive remedy as a drug releasing agent, since it is highly stable in organic medium and it slowly decomposes to curcumin in aqueous organic medium. Siu et al. observed that Rubrocurcumin is active against HIV protease and its hydrolyzed product is a well-established biological active reagent [14]. To the best of our knowledge, this is the first study evaluating the metal complex of naturally occurring bioactive food compound, curcumin on skin cancer cells. Due to the special structure of this compound, an increase in bioavailability and biostability is attributed. The findings of this study would pave newer ways for site directed cancer therapy, by suggesting Rubrocurcumin as a suitable drug candidate.
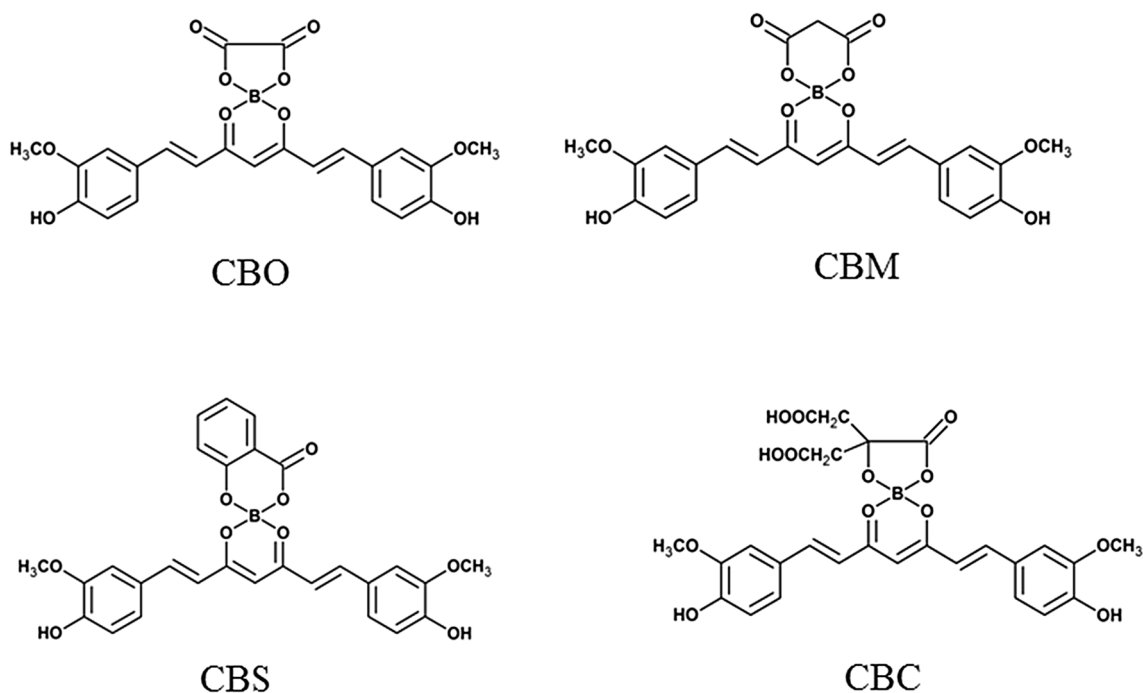

Fig. 1 The chemical structure of synthesised spiroborate complex of Curcumin with oxalic acid (CBO), Malonic acid (CBM), salicylic acid (CBS), Citric acid (CBC)

Materials and methods

All chemicals and reagents used were of analytical grade. All biochemical kits were purchased from M/s Sigma, USA. The cell lines used in the study A431, (skin cancer cells) were procured from NCCS Pune, MCF-7 (breast cancer cells) from RGCB, Poojapura and normal cell (3T3L1) was procured from Department of Biotechnology, University of Kerala. The ethical approval for this study has been sought from the Institute Animal Ethics Committee (IAEC), University of Kerala, sanction No. IAEC-KU-1/2014-15-BC-AA (38).

The synthesis of spiroborate esters

Curcumin which was separated from commercial sample of curcuminoids using silica gel column chromatography [15] is used for the synthesis of spiroborate esters of curcumin. A mixture of curcumin (0.01 M), boric acid (0.01 M) and the dicarboxylic acid (oxalic acid, malonic acid)/hydroxy acid (salicylic acid, citric acid) (0.01 M) in 10 mL toluene were stirred for 3–5 h at 90–100 °C. The formation of complex was monitored through Thin Layer Chromatography (TLC) and after the completion of the reaction the solvent was removed by filtration to get the solid product. It was further washed with toluene to remove unreacted curcumin and recrystallized from acetone. The organic structure of the synthesised molecules is depicted in Fig. 1.

Stability and drug selection studies

The stability and degradation of the synthesised drug complexes, spiroborate complex of curcumin with (A) salicylic acid (CBS), (B) citric acid (CBC), (C) malonic acid (CBM), oxalic acid (CBO) were studied in acqueous medium like Dulbecco's Modified Eagle's Medium for different time intervals (2 h, 3 h, 4 h, 24 h) and the absorption spectra was determined using UV–Vis spectrophotometer. Also the morphological changes in cancer cell line upon addition of drug (300 μg) was noted for selection of the most anti-cancer effect for further in vitro studies.

Spectroflurimetric analysis of compound

The fluorescent property of the selected drug complex (Rubrocurcumin, CBO) was checked by measuring the emission spectra by a spectroflurimeter.

Cellular uptake studies

The internalization of drug complex (Rubrocurcumin, CBO) was examined in A431 cells by using fluorescence microscopy. Drug has a fluorescent property, so we used this drug for cell imaging and further checked the cellular uptake of this material. Cells were seeded at a density of 5×10^4 cells/mL and allowed to incubate at 37 °C for 24 h in culture medium supplemented with 10% FBS. After incubation the cells were treated with drug for 24 h, washed with PBS and further analysed the cellular uptake.

Cytotoxicity assays

Cytotoxicity in 3T3L1 adipocytes and MCF7, A431 cancer cells

Toxicity of the drug complex (Rubrocurcumin, CBO) to a normal cell line, *3T3L1* adipocytes and cancer lines, MCF7, A431 was studied by culturing the cells with different concentration of the drug for different time intervals. The assays used to determine cytotoxicity were MTT, NRU and LDH leakage assays. Also nuclear condensation studies by Hoechst staining ewas carried out. Qualitative evaluation of cytotoxicity like observation of changes in cell morphology and adherence was also noted.

MTT cell proliferation assay [16] Cells were seeded in to 96 well microtetraplate (5000 cells/well) in 10% DMEM and incubated for 24 h. Once the cells have attached, drug was added in different concentration (100–300 μg/ml) in duplicate and incubated for different time intervals (24, 48, 72 h) at 37 °C. Cells treated with 10 mM concentration of cisplatin were taken as positive control and another set maintained without any treatment as control. After incubation, at each time interval the medium was removed and equal volumes of fresh medium were added along with 20 ml MTT (5 mg/ml) to each well. The plates were kept for 3 h incubation. The yellowish MTT was reduced to dark coloured formazan by viable cells only. The formazan crystals formed were solubilized with MTT lysis buffer (20% SDS in 50% dimethyl formamide). The plate was kept protected from light, overnight at 37 °C in an incubator. The color developed was quantitated with ELISA plate reader (BioRad systems, USA) measuring at wavelength 570 nm.

The cells survival (CS) expressed as percentage was calculated as follows.

$$CS = (OD \text{ drug exposed cell/mean OD control wells}) \times 100$$

The graph was plotted by taking percentage viability in the y-axis and concentration of drug in the x-axis.

Neutral red uptake (NRU) assay [17] Cells were treated with different concentration of drug (100–300 µg/ml) in duplicate and incubated for different time intervals (24, 48, 72 h) at 37 °C. After incubation, a solution of neutral red, a vital dye was added to the 96 well plates. The plates were incubated at standard culture conditions to allow neutral red uptake by the cells. After 2 h incubation, decanted excess neutral red and PBS was added to the wells. The solvent extracts the neutral red dye contained within the cells. The plates were placed on a plate shaker to fully extract the neutral red and evenly distribute the dye in each well and absorbance with a 540 nm was measured using a micro plate reader (BioRad, USA). The absorbance value (optical density) are then used to determine the viability of each well comparing the optical density of the each material treated well compared the negative control well.

LDH cytotoxicity assay [18] This is a colorimetric assay that quantitatively measures LDH, a stable cytosolic enzyme that is released into the culture medium upon cell damage or lysis occurs during both apoptosis and necrosis [18]. LDH catalyzes the reduction of NAD+ to NADH and H+ by oxidation of lactate to pyruvate, which in turn catalyze the reduction of a tetrazolium salt to a colored formazan and the absorbance of the formazan developed can read at 490 nm. The amount of formazan produced is proportional to the amount of LDH released into the culture medium.

Cells were added in 24 well plates, exposed to drug conjugated gold nanoparticle with different concentration (100–300 µg/ml) and incubated for different time intervals (24, 48, 72 h). After incubation the cell suspension was centrifuged at 4000 rpm for 5 min and transferred to 100 ml of the supernatant to each well in a microplate. Then added 100 µl of reaction solution to each well and incubated plates with gentle shaking for 30 min at room temperature. Read the absorbance at 490 nm using a plate reader (BioRad, USA).

$$A_{test} = (A_{control} + A_{lysed}) \times 100$$

LDH activity can be determined by plotting a graph against absorbance in y axis and time interval in x axis.

Nuclear staining analysis—Hoechst staining Chromatin condensation is a late apoptotic event, which can be determined by Hoechst staining. Hoechst 33342 is a DNA binding, non-intercalating, benzimidazole derivative dye that binds differentially to A-T rich regions of DNA. This dye is excited by UV light at 395 nm and emits blue fluorescence at 450 nm. Transport of Hoechst across the plasma membrane is altered in apoptotic cells. Dye is diluted in the buffer in the ratio 1:1000. The cells were grown in 96 well plates and apoptosis was induced in them by addition of specific drugs and kept for incubation at 37 °C for 24 h. After incubation the cells were taken from CO_2 incubator and medium was discarded and diluted dye was added to the wells. The cells were then incubated at 37 °C for 15 min in CO_2 incubator and were observed under the microscope.

Cell cycle analysis by FACS

The most commonly used dye for DNA content for cell cycle analysis is propidium iodide. Propidium iodide is a red colour stain which is used for cell cycle analysis to determine in which is used for cell cycle analysis to determine in which phase of the cell cycle, the arrest is occurring. It intercalates with major groove of DNA strand and produces highly fluorescent adduct which can be excited at 488 nm with a broad emission entered on 600 nm, Since PI can also intercalate with RNA, it is necessary to treat the cells with RNase for optimal DNA resolution. For FACS analysis, the cells were seeded in 12 well plates and the drugs were added to the respective wells having sufficient cell density. After 24 h of drug treatment the cells were harvested with trypsin and collected in FACS tubes. These tubes were centrifuged at 3500 rpm at 4 °C for 7 min, the supernatant was discarded and the pellet was resuspended in 1 ml of ice cold 1× PBS. Then the tubes were again centrifuged at 3500 rpm at 4 °C for 7 min. The pellet was dissolved in 0.3 ml of ice clod 1× PBS, this was followed by the addition of 0.7 ml cold 70% ethanol, ethanol was added drop wise while vortexing gently. Then kept the tubes for 45 min, again centrifuged the tubes at 3500 rpm at 4 °C for 7 min. Then the pellet was resuspended in 0.25 ml 1× PBS this was followed by the addition of 5 µl of RNase into each tube, the tubes were incubated 37 °C for 30 min. Then added 5 µl of PI stain into each tube, the tubes were kept in dark for 5 min. Using 0.75 µl filter, the suspension was filtered after diluting with 1× PBS, the tubes were then loaded for analysis in a flowcytometer.

Results

Synthesis and stability of spiroborane complexes

The synthesis and spectroscopic identification of spiroborate ester formed from oxalic acid (CBO) and salicylic acid (CBS) were reported recently elsewhere [11, 17]. The structure of CBM was confirmed by the spectral data which corresponds to that reported by Sui et al. [14]. The spectral data of CBS correspnds to the methyl derivative of C was reported earlier [19].

Spectral details of CBM and CBS

CBM

Yield 80%; UV $\lambda_{max} = 516$ nm (acetonitrile); IR (KBr): 3512 (OH), 1670 (C=O in lactone ring), 1513 (C=O in curcumin), 1207(C–O in phenol),1058 cm^{-1} (C–O in OCH$_3$); ^{1}H NMR (400 MHz, DMSO-d6); δ 3.84 (s, 6H, OCH$_3$), 3.70 (s, 2H,CH2) 6.48 (s, 1H, CH), 7.36 (d, J = 10 Hz, 2H, Ar–H), 6.89 (d, J = 8 Hz, 2H, Ar–H), 7.45 (s, 2H, Ar–H), 8.02 (d, J = 15.6 Hz, 2H, =CH), 7.07 (d, J = 15.6 Hz, 2H, =CH), 10.175 (s, 2H, OH); ^{13}C NMR: 55.76, 100.47, 112.59, 116.03, 117.30, 125.73, 126.01, 148.21, 148.27, 151.86, 165.55, 177.58.

CBS

Yield 75%; UV $\lambda_{max} = 500$ nm (acetonitrile); IR (KBr): 3468 (OH), 2888 (C–H), 1725 (C=O in lactone ring), 1553 (C=O in curcumin), 1289 (C–O in phenol), 1081 cm^{-1} (C–O in OCH$_3$); ^{1}H NMR (400 MHz, DMSO-d6); δ 2.73–2.83 (m, 4H, CH$_2$), 3.8 (s, 6H, OCH$_3$), 6.43 (s, 1H, CH), 7.32 (d, J = 10 Hz, 2H, Ar–H), 6.89 (d, J = 8.4 Hz, 2H, Ar–H), 7.43 (s, 2H, Ar–H), 7.90 (d, J = 15.2 Hz, 2H, =CH), 7.01 (d, J = 15.6 Hz, 2H, =CH), 10.09 (s, 2H, OH), 12.188 (s, 2H, COOH); ^{13}C NMR: 42.88, 55.80, 78.33, 100.91, 111.94, 115.86,117.99, 125.57, 126.62, 147.03, 148.19, 151.30, 170.40, 176.66, 178.59.

In water mediated condition all spiroborate esters get hydrolysed to yield curcumin which is clearly observable by the decrease in absorption peak of these complexes at its λmax and the increase in peak at 420 nm due to the formation of curcumin. The decrease in peak at its λmax is monitored spectrophotometrically and the rate of decomposition observed is first order with respect to the

Table 1 The rate constant of the hydrolysis of spiroborate esters in 20% aqueous acetone at 50 °C

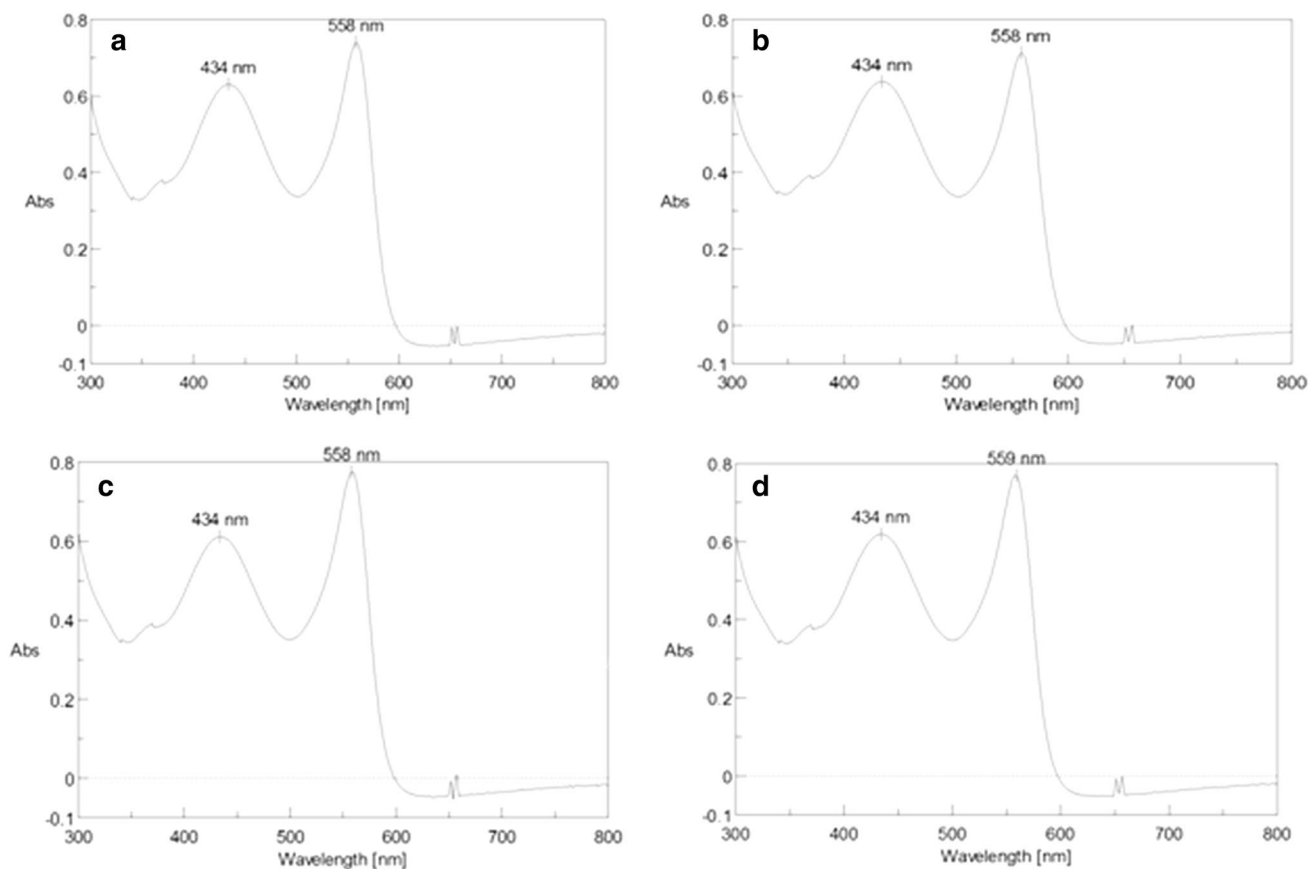| Compound	10^5 k (s^{-1})	T½ (h)
CBO	12.23	1.5
CBM	16.33	1.1
CBC	30.71	0.6
CBS	93.54	0.2

Fig. 2 Stability study of Rubrocurcumin in DMEM **a** after 1 h, **b** 2 h, **c** 4 h, **d** 24 h

substrate. The rate constant of the hydrolysis of spiroborate esters in 20% aqueous acetone at 50 °C is given in Table 1. The Rubrocurcumin (CBO), (curcumin, boric and oxalic acid compound) is the most stable compound among the synthesised spiroborate esters (Fig. 2). At lower temperature the rate of decomposition decreases and at 25 °C in 50% acetone the half life of CBO is 228 h and expected to be stable in most of the biological conditions.

The Rubrocurcumin (CBO), the most stable compound among the synthesised spiroborate esters is very active against the cancer cell lines used in the preliminary study (Fig. 3d).

The complexes may have a different stability in the medium of study and their stabilities were studied for 24 h. The complexes were sufficiently stable for the biolological studies condition as shown by Rubrocurcumin in the culture medium DMEM in Fig. 2.

The morphological changes observed for cancer cell line upon addition of the synthesised spiroborate esters (100 μg) were depicted in Fig. 3. The maximum cell death was observed for CBO (Fig. 3d) which is found to be the
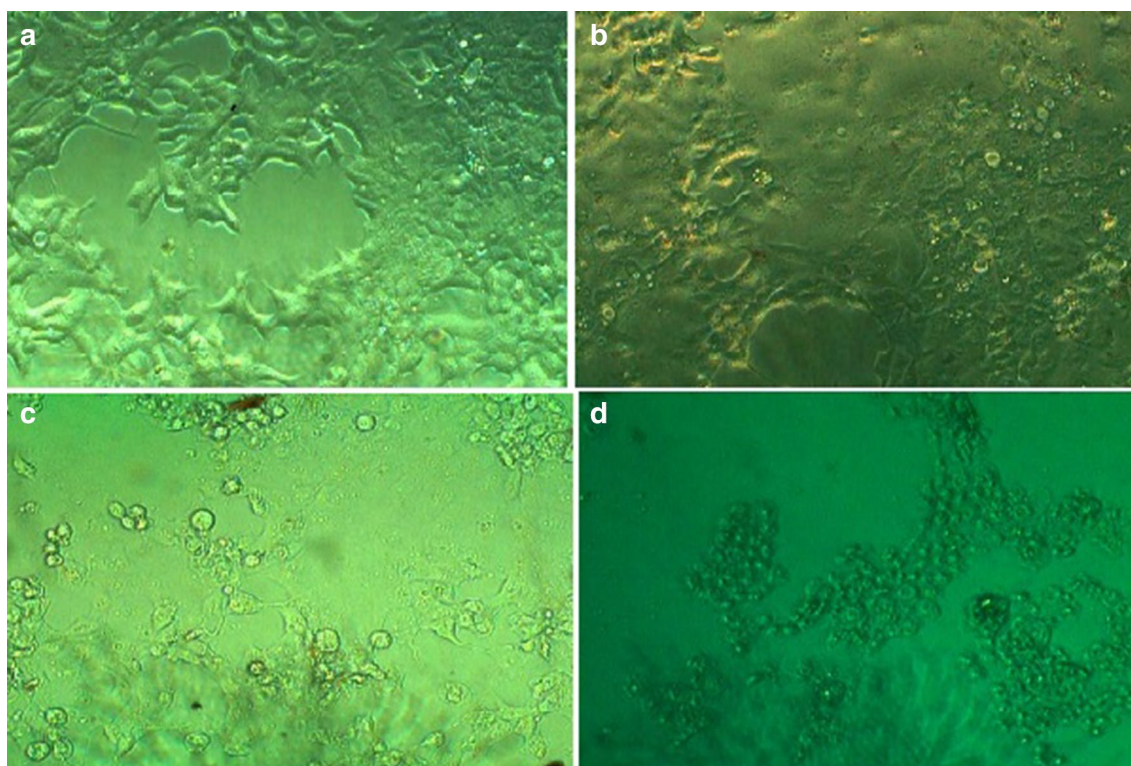

Fig. 3 Morphological changes of cancer cells upon addition of 100 μg of **a** CBS, **b** CBC, **c** CBM, **d** CBO and **e** cisplatin (10 μM/ml) after 24 h of incubation
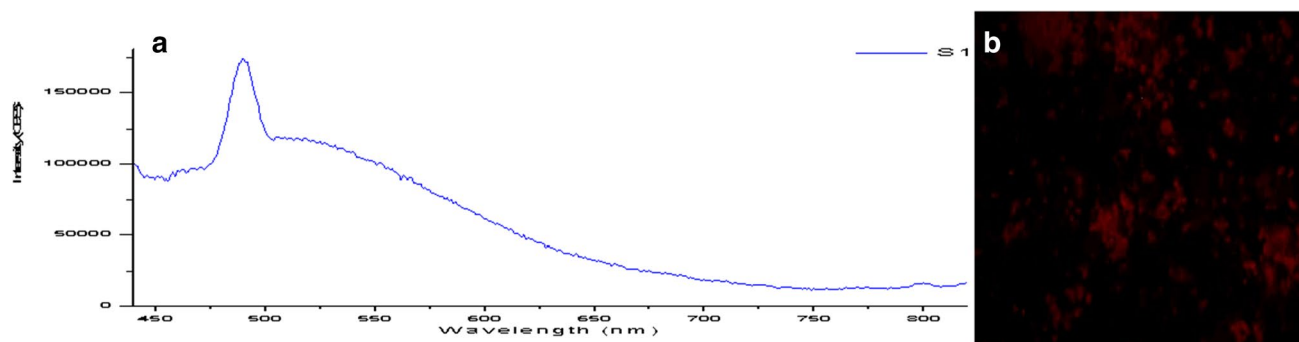

Fig. 4 Spectroflurimetric analysis of the CBO (**a**) and its cellular uptake (**b**)

most stable in water mediated condition and selected for further in vitro studies.

Spectro flurimetric analysis of the compound

The drug CBO is fluorescent in nature as shown by the fluorescence spectrum shown in Fig. 4, the maximum emission was observed at 460 nm (Fig. 4a).

Cellular uptake studies

Cellular uptake studies confirmed the intracellular presence of the drug within the A431 cells (Fig. 4b), after 24 h of incubation with cancer cell lines.

Cytocompatibility assays in 3T3L1 adipocytes and MCF7 and A431 cancer cells

Toxicity of CBO in normal cells 3T3L1 adipocytes are carried out at different time intervals by MTT, NRU, and LDH leakage assay and are presented in Fig. 5a–d. Studies show that the drug is compatable with normal 3T3L1 adipocytes as shown by more than 80% cells viability in MTT and NRU assay and least LDH activity even after 72 h of incubation.

On morphological analysis, the cells did not show any morphological changes (Fig. 5d).

The cytotoxicity assay results of CBO treated MCF-7 cancer cells are presented in Fig. 6. In MTT assay a concentration depended activity was observed. A 100 μM/ml reduces the cell viability to 45% and at 300 μM/ml the viability reduces to 32% however is less than that of standard ant-cancer drug, cisplatin (10 mM/ml concentration of cisplatin). Time dependent cell viability is comparatively less indicating active drug interaction within 24 h of incubation. Similar results are observed for NRU assay (Fig. 6b) where 60–40% cell viability is observed for 24 h treatment of drug in 100 μM/ml to 300 μM/ml. The time dependence has more influence for NRU assay than MTT assay. (Fig. 6a).

The LDH assay on MCF-7 cancer cells revealed that there is increased release of LDH, when drug is treated with cancer cell rather than the normal cell. For normal cell the absorption value is < 0.1 at different times of incubation (Fig. 5c), however with cancer cell a concentration depended release of LDH is observed which ranges from 0.05 to 0.8 (Fig. 6c). The LDH release increases with the longer times of incubation.

The morphological variations of MCF-7 cells on treatment with CBO are presented in Fig. 7. The control cells did not show any morphological changes (Fig. 7a) but
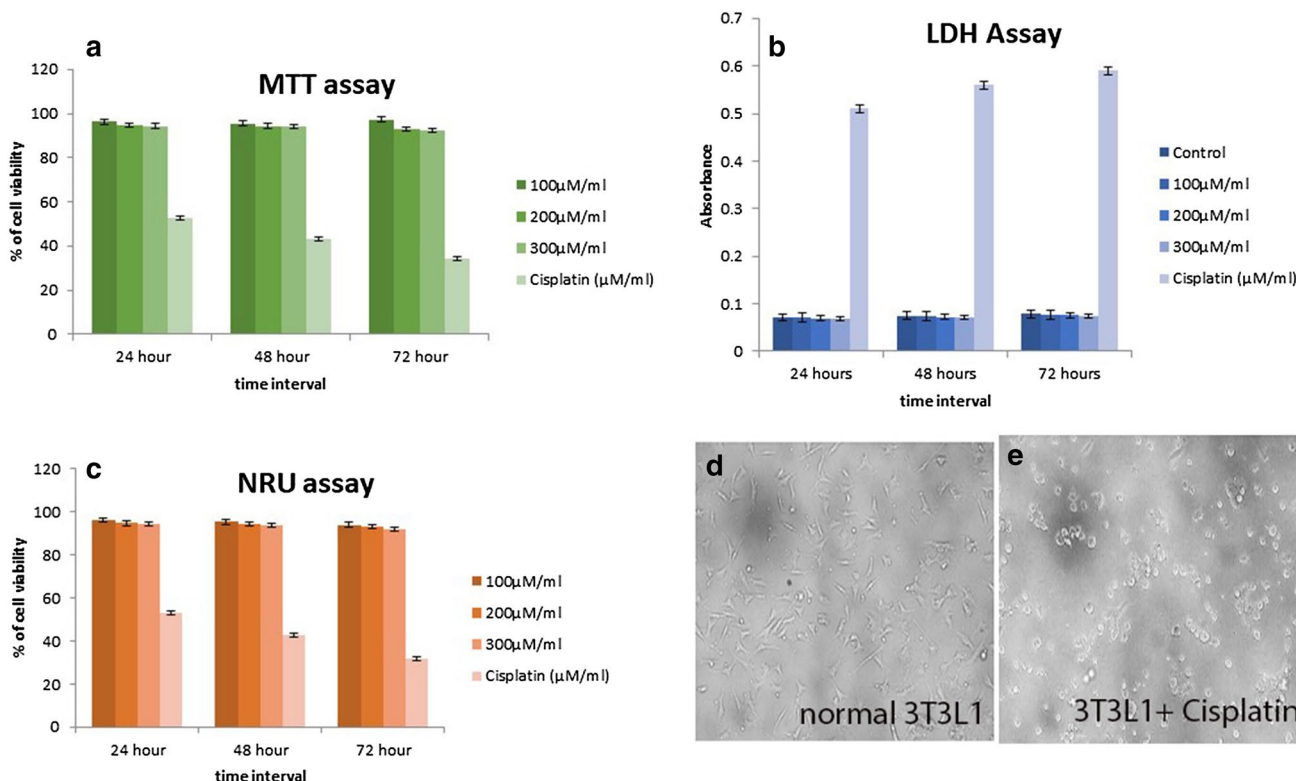

Fig. 5 Cytocompatability evaluation of the CBO on 3T3 adipocytes, **a** MTT assay, **b** neutral red assay, **c** LDH assay, **d** normal 3T3L1 adipocytes, **e** cisplatin treated 3T3L1 adipocytes. The results of **a, b** and **c** are mean ± SD, n = 6, p ≤ 0.05
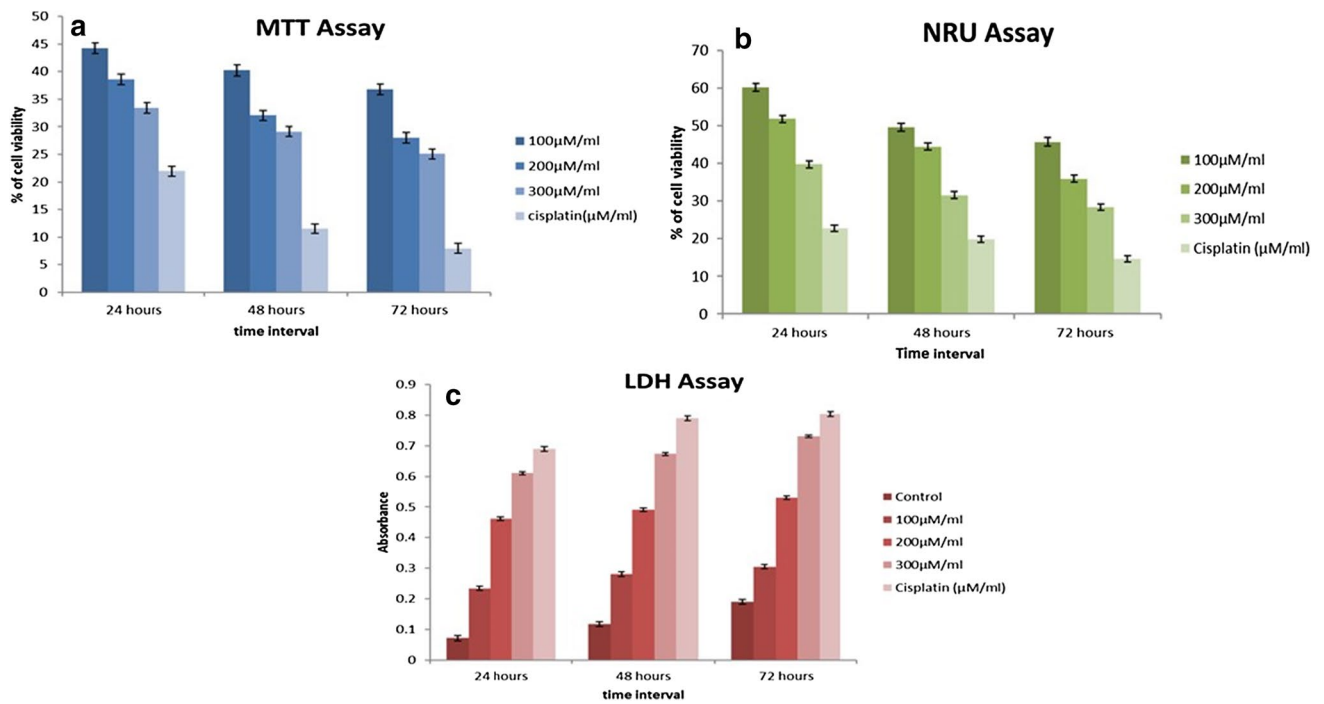
Fig. 6 Cytotoxicity assays of the CBO on MCF-7 cancer cell line. **a** MTT assay, **b** neutral red assay, **c** LDH assay. The results of **a, b** and **c** are mean $\pm$ SD, n = 6, p $\leq$ 0.05
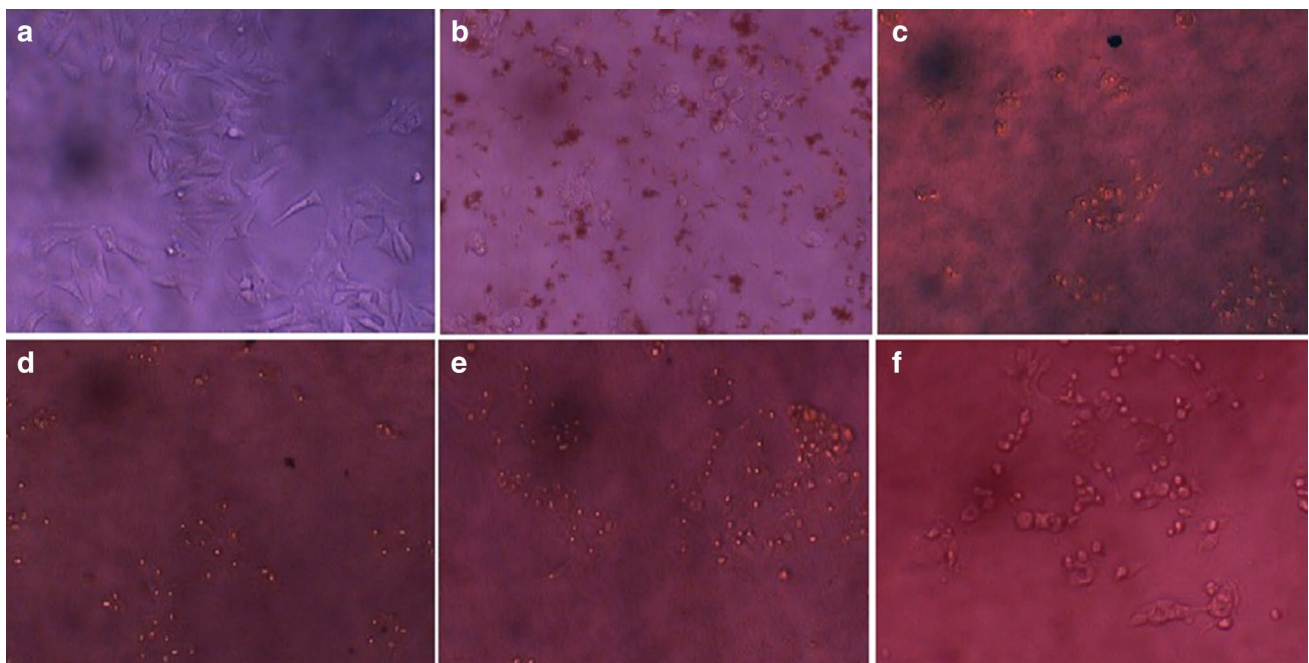

Fig. 7 Morphological changes of MCF-7 cell line after 24 h incubation of CBO treatment: **a** control cells; **b** cells treated with curcumin 200 μM/ml; **c** cells treated with 100 μM/ml CBO; **d** cells treated with 200 μM/ml CBO; **e** cells treated with 300 μM/ml CBO, and **f** cells treated with 10 μM/ml cisplatin (positive control)
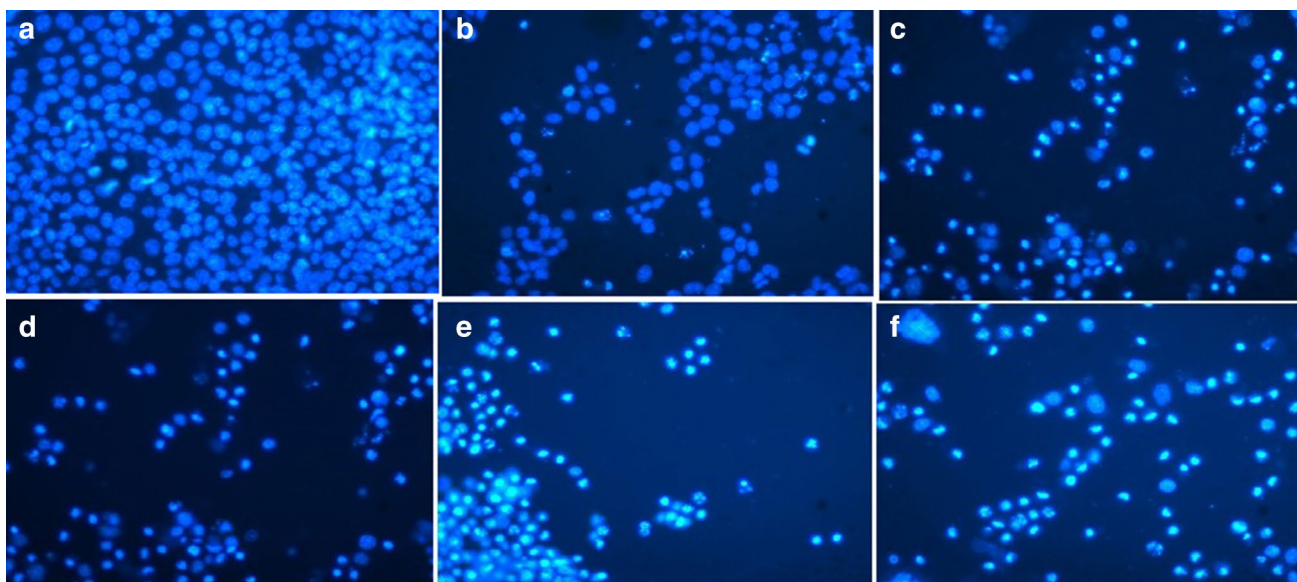
Fig. 8 Hoechst staining of MCF-7 after CBO addition **a** control cells; **b** treated with standard curcumin 200 μg/ml; **c** treated with 100 μg/ml CBO; **d** treated with 200 μg/ml CBO; **e** treated with 300 μg/ml CBO; and **f** treated with 10 μg/ml cisplatin (positive control)

CBO treated cells were in irregular confluent aggregates with round and polygonal cell morphology (Fig. 7c–f).

In curcumin and CBO treated MCF-7, destruction of monolayer was observed. The treated cells with normal polygonal morphology after 24 h of incubation, began to shrink and became spherical in shape (Fig. 7b, e). The cell shrinkage increased progressively in dose and time dependent manner. This shrinkage may be due to the growth inhibitory effect of compound.

Nuclear staining analysis—Hoechst staining

The images of Hoechst staining of MCF-7 cells are presented in Fig. 8 which shows that the nuclear condensation pattern increases with the CBO treated cells in a concentration depended manner. More condensation is observed for CBO than curcumin. At 300 μg CBO addition, the cells show condensation pattern similar to the standard drug cisplatin treated cell after 24 h (Fig. 8e).

Cytotoxicity evaluation by MTT, NRU, LDH of different concentration of CBO addition to A431 cells shows that at CBO-300 μg, maximum cell death was observed (Fig. 9a–c).

The results of CBO addition at various concentrations to A431 skin cancer cells resulted in irregular confluent aggregates of cells with round and polygonal morphology (Fig. 10c–e). The result was comparable to that in cisplatin treated group (Fig. 10f).

Cell cycle analysis by FACS

When cell suspension is subjected to flow cytometry, it illuminates the cells when they flow individually in front of a light source and lead to detection, counting and sorting of the cells. In order to analyze the apoptosis induced by this drug complex, we treated the cancer cells with CBO at different concentrations for 24 h.

The histogram showed that at 300 μg drug concentration, highest cell population underwent cell cycle arrest at G_0 phase (cell death occur at G_0 phase) (Fig. 11d), confirming that A431cells are sensitive to the cytotoxic action of this novel drug complex.

Discussion

Today it is alarming to note that cancer is the record leading cause of death across the world [3]. It is very clear that the conventional cancer therapies result in serious side effects, further extending patient's life span rather giving permanent cure. Hence, arise the demand to utilize alternative concepts or approaches for the treatment of 'emperor of all maladies'. There is compelling evidence signifying the role of natural compounds in inhibiting the development and spread of tumors in experimental animals [20]. Well standardised traditional natural products have long been used to prevent and treat many diseases and thus they are promising candidates for the development of anti-cancer drugs [21]. Discovery of
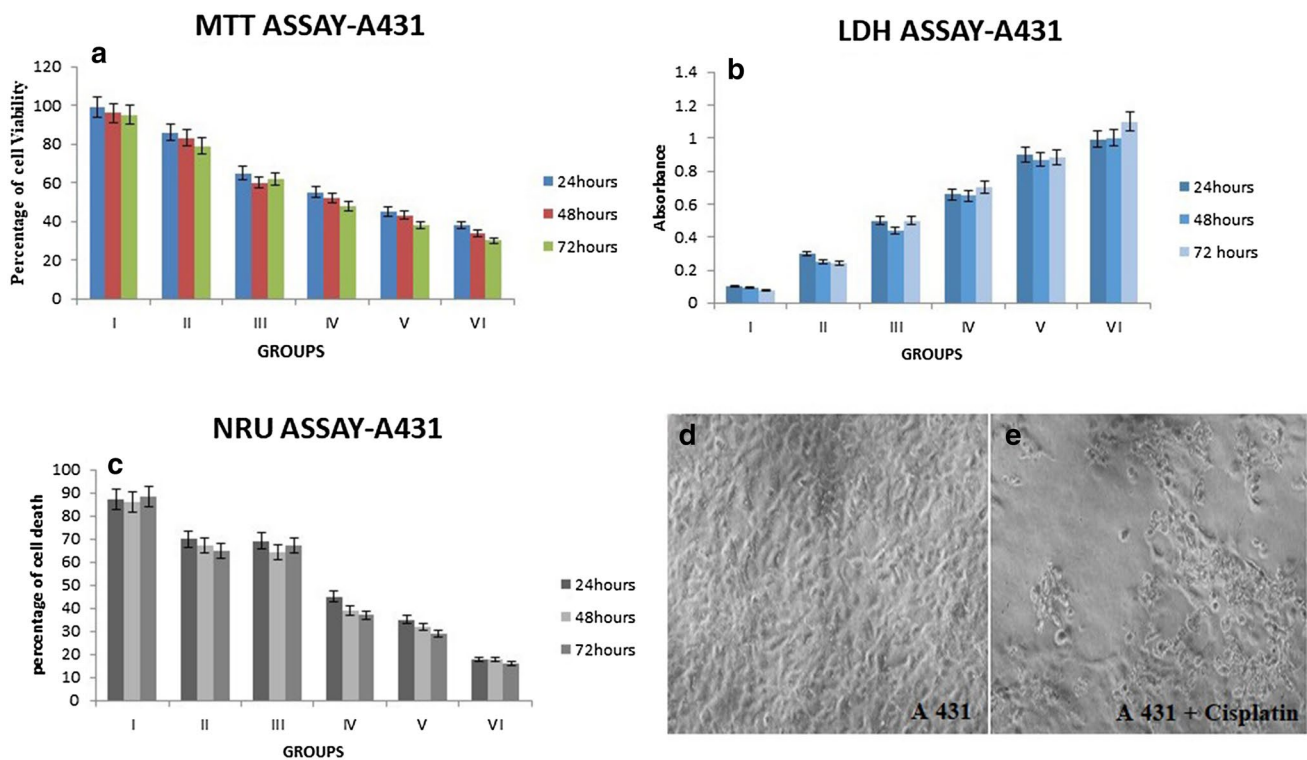
Fig. 9 Cytotoxicity assays of the drug on A431 skin cancer cell line. **a** MTT assay, **b** neutral red assay, **c** LDH assay. The results of **a, b** and **c** are mean ± SD, n = 6, p ≤ 0.05. **d** normal A431 cells, **e** Cisplatin treated A431 cells
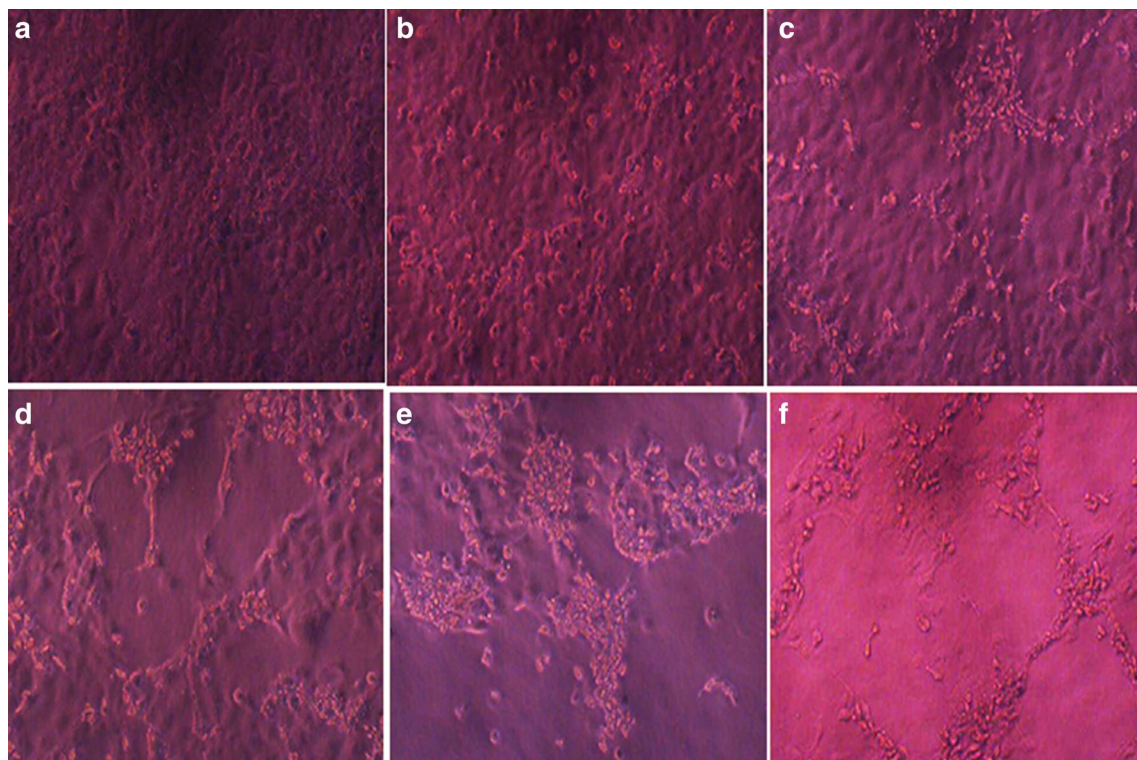

Fig. 10 Morphological changes of A431 cell line after 24 h incubation of CBO treatment. **a** Control cells; **b** cells treated with 200 μM/ml standard curcumin; **c** cells treated with 100 μM/ml CBO; **d** cells treated with 200 μM/ml CBO; **e** cells treated with 300 μM/ml CBO; and **f** cells treated with 10 μM/ml cisplatin (positive control)
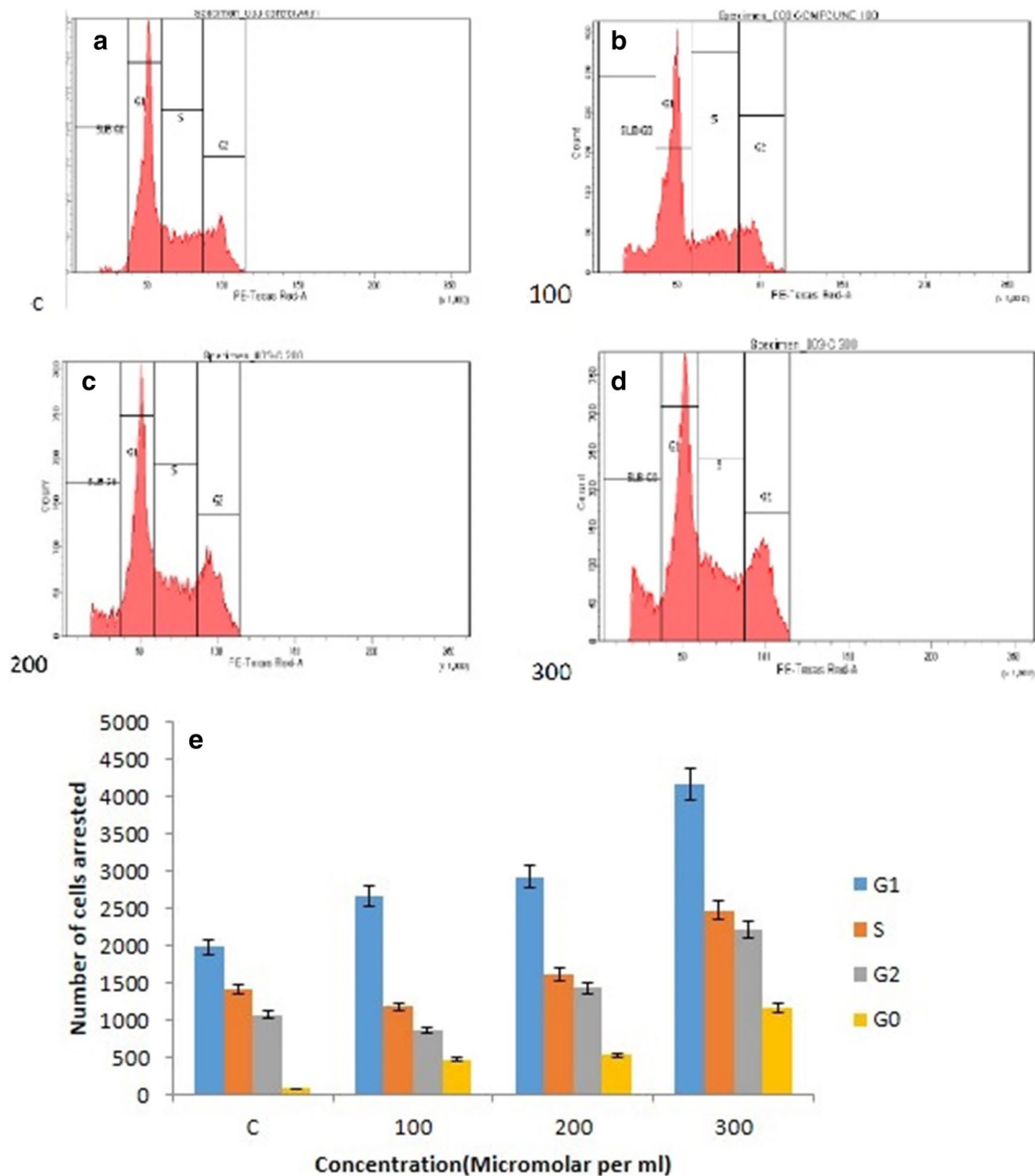
Fig. 11 Flow histogram of A431 cells added with CBO: **a** control; **b** treated with 100 μg/ml; **c** treated with 200 μg/ml; **d** treated with 300 μg/ml (maximum cell death at 300 μg/ml); and **e** quantification analysis of flow histogram

active compounds from natural products with the potential for use as chemotherapy and/or chemotherapeutic agents are of great interest for cancer treatment. Though chemotherapy is largely used for treatment of cancer, it is found that the results are not always satisfactory necessitating the need for new and effective methods of treatment. Hence this study, we have made an attempt to synthesise and screen novel biostable curcumin derivative drugs (spiroborate esters of curcumin with oxalic acid, citric acid, malonic acid and

salicyclic acid) and validate the most stable drug complex, rubrocurmin's (spiroborate ester of curcumin with oxalic acid) anticancer properties in in vitro models [22].

As a hydrophobic functional food polyphenol isolated from dried rhizomes of turmeric (*Curcuma longa* Linn.), curcumin has various pharmacological activities including anti-oxidant, anti-bacterial, anti-fungal, anti-viral, anti-inflammatory and anti-cancer properties. Cancer is a hyper proliferative disorder affecting the vital organs

of the body through invasion and angiogenesis. The last four decades have seen great medicinal advances in the treatment of cancer exploiting different biochemical pathways. Cancer fundamentally alters the normal cellular and molecular events of affected cells. These altered cells divide and grow in the presence of signals that normally inhibit cell growth [23] but in cancer they do not require special signals to induce cell growth and division. Hence, the significance of natural curcumin and curcumin conjugated products which could block the transformation, proliferation, and invasion of tumor cells [24].

In our study, the stability of the curcumin derived drug complexes were studied by UV–Vis spectrophotometry and the compound, Rubrocurcumin, the spioborate ester of curcumin with oxalic acid was found biostable in the DMEM medium (Fig. 2). This corroborates with the earlier reports of Bernabe-Pineda et al. [25]. In a separate report, Souza and co-workers [26] also studied the influence of water activity on the stability of curcuminoid pigments in curcumin- and turmeric oleoresin–microcrystalline–cellulose model systems. Wang et al. examined the degradation kinetics of curcumin under various pH conditions and the stability of curcumin in physiological matrices [27].

As this CBO, is a newly synthesised compound and its cytocompatibility and anticancer effects have not been studied earlier and since it has translational potential, we checked initially the cytotoxicity of CBO in normal cell line, 3LT31 adipocytes. Since we expect the efficacy of this novel compound against the major types of skin cancers, we have tested the anticancer effect in two different cell lines i.e., MCF-7 and A431, both of which have a common epithelial origin. The anti-cancer effects of the spiroborane complex of curcumin (Rubrocurcumin) was confirmed from the in vitro morphology changes (Figs. 7, 10), toxicological assays such as MTT, neutral red, LDH assays (Figs. 5, 6, 9) and nuclear chromatin condensation by Hoechst staining (Fig. 8). On morphological analysis, control cells did not show any morphological changes, but CBO treated cells were observed as irregular confluent aggregates, shrinked with round and polygonal morphology. This shrinkage might be due to the growth inhibitory effect of compound.

MTT assay is a colorimetric method effectively used to screen the cell proliferation and cytotoxicity of drugs. The MTT test assesses the cell metabolism based on the ability of mitochondrial succinate hydrogenase to convert the yellow compound, 3-(4, 5-dimethylthiazol-2-Yl)-2, 5-diphenyltetrazolium bromide (MTT) to a blue formazan dye. The amount of dye produced is proportional to the number of live and metabolically active cells. In this study, we observed that percentage of viability in MCF-7 cells decrease with increase in concentration of the drug (Fig. 6a). This has been compared with the standard cytotoxic drug, cisplatin

(10 μM/ml) based on the earlier reports proving 100% anti-proliferative activity against cancer cell lines [28, 29].

One of the main advantages of neutral red (NR) dye is that it readily penetrates into cell membranes through non-ionic diffusion and the dye accumulates intracellularly in lysosomes. Alterations of the cell surface or the sensitive lysosomal membrane lead to lysosomal fragility and other changes that gradually become irreversible. Such changes result in decreased uptake and binding of NR, thereby aiding distinction between viable, damaged, or dead cells; which is the basis of this assay. Thus it provides a quantitative estimation of the viability of cells in culture. In this study, it was observed that NRU uptake increases with the time of incubation and the uptake was proportional to the concentration of the NRU solution and the number of viable cells (Fig. 6b).

Lactate dehydrogenous (LDH) is a cytoplasmic enzyme which catalyses the inter conversion of NADH and NAD$^+$. It converts pyruvate, the final product of glycolysis to lactate when oxygen is absent or in short supply, and it performs the reverse reaction during the cori cycle in the liver. LDH released into the culture medium when cell damage or lysis occurs during apoptosis/necrosis. LDH activity is an indication of cell membrane integrity, otherwise an indirect measure of cytotoxicity. LDH catalyses the reduction of a tetrazolium salt to coloured formazan and the absorbance of the formazan developed can be read at 490 nm. The amount of formazan produced is proportional to the amount of LDH released into the culture medium. In this study, we observed that the percentage of viability in MCF-7 cells increases with increase in concentration (Fig. 6c).

Hoechst staining is employed to study the chromatin condensation (Fig. 8). Nuclear chromatin condensation is one of the hallmarks of apoptosis. Both intrinsic and extrinsic signaling culminates ultimately in nuclear chromatin condensation and causes cell death. Cytotoxicity evaluation by MTT, NRU, LDH of different concentration of CBO addition to A431 cells shows that at CBO-300 μg, maximum cell death was observed (Fig. 10b–f).

In order to analyze the apoptosis induced by the cytotoxic agents, we treated the cells with the compound in different concentrations for 24 h, analysed by flow cytometer and found that cell cycle was arrested (Fig. 11). In flow cytometry, the measurements were made as the cells or particles pass through the flow cytometry, in a liquid stream. The results showed that A431 cells are sensitive to this novel drug complex.

Another interesting observation is the fluorescent property of this compound, which was confirmed by spectroflurimetric analysis. It showed the maximum emission at 460 nm (Fig. 4a). This inherent fluorescence suggests this rubrocurmin complex as a novel candidate for targeted drug delivery due to the easiness in in vivo tracking. In future, we intend to incorporate this drug in nano metal like Au (gold)

to increase its further availablity and target effectiveness. Uptake of this fluorescent drug complex intracellularly is a crucial data for pursuing future modifications (Fig. 4b). Thus the results from our in vitro screening studies supports the anti-cancer, biostable, fluorescent properties of novel spiroborate complex of curcumin (Rubrocurcumin). Since the drug is biostable and degrades in vivo to harmless products and get eliminated from body (unpublished data), we could strongly suggest this drug as an alternate safe source for currently used chemotherapeutics.

Conclusion

The results from this in vitro study proposes the spiroborate complex of curcumin, Rubrocurcumin as a novel anti-cancer drug which is biostable and has inherent fluorescent property. This drug with its chemotherapeutic and tracking properties could be used as a molecular drug for site directed therapy in cancer patients. Further pre-clinical studies in in vivo models are warranted.

Compliance with ethical standards

Conflict of interest The authors confirm that there are no known conflicts of interest associated with this publication.

References

1. Siegel RL, Miller KD, Jemal A (2017) Cancer statistics, 2017. CA Cancer J Clin 67:7–30
2. Tang L, Wang K (2016) Chronic inflammation in skin malignancies. J Mol Signal 11:2
3. Torre LA, Bray F, Siegel RL, Ferlay J, Lortet-Tieulent J, A. Jemal (2015) Global cancer statistics, 2012. CA Cancer J Clin 65:87–108
4. Phillips JM, Clark C, Herman-Ferdinandez L, Moore-Medlin T, Rong X, Gill JR, Clifford JL, Nathan AF (2011) Curcumin inhibits skin squamous cell carcinoma tumor growth *in vivo*. Otolaryngol Head Neck Surg 145:58–63
5. Sonavane K, Phillips J, Ekshyyan O, Moore-Medlin T, Gill JR, Rong X, Lakshmaiah RR, Abreo F, Boudreaux D, Clifford JL, Nathan CAO (2012) Topical curcuminbased cream is equivalent to dietary curcumin in a skin cancer model. J Skin Cancer. https://doi.org/10.1155/2012/147863
6. Ravindran J, Prasad S, Aggarwal BB (2009) Curcumin and cancer cells: how many ways can curry kill tumor cells selectively? AAPS J 11:495–510
7. Park W, Amin AR, Chen ZG, Shin DM (2013) New perspectives of curcumin in cancer prevention. Cancer Prev Res 6:387–400
8. Hodges RE, Minich DM (2015) Modulation of metabolic detoxification pathways using foods and food-derived components: a scientific review with clinical application. J Nutr Metab. https://doi.org/10.1155/2015/760689
9. Lee WH, Loo CY, Bebawy M, Luk F, Mason RS, Rohanizadeh R (2013) Curcumin and its derivatives: their application in neuropharmacology and neuroscience in the 21st century. Curr Neuropharmacol 11:338–378
10. Wanninger S, Lorenz V, Subhan A, Edelmann FT (2015) Metal complexes of curcumin—synthetic strategies, structures and medicinal applications. Chem Soc Rev 7:4986–5002
11. Jeena J, Sudha Devi J, Balachandran SN (2017) Kinetic analysis of thermal and hydrolytic decomposition of spiroborate ester of curcumin with salicylic acid. Orient J Chem 33:849–858
12. Jeena J, Sudha Devi R, Balachandran S (2016) Kinetic analysis of thermal decomposition of rubrocurcumin. Acta Clienta Indica XLII C 2:121
13. Kornhauser A, Coelho SG, Hearing VJ (2010) Applications of hydroxy acids: classification, mechanisms, and photoactivity. Clin Cosmet Investig Dermatol CCID 3:135–142
14. Sui Z, Salto R, Li J, Craik C, Ortiz de Montellano PR (1993) Inhibition of the HIV-1 and HIV-2 proteases by curcumin and curcumin boron complexes. Bioorg Med Chem 1:415–422
15. Asha R, Devi RS, Priya RS, Balachandran S, Mohanan PV, Abraham A (2012) Bioactive derivatives of curcumin attenuate cataract formation in vitro. Chem Biol Drug Des 80:887–892
16. Mosmann T (1983) Rapid colorimetric assay for cellular growth and survival: application to proliferation and cytotoxicity assays. J Immunol Methods 65(1–2):55–63
17. Lasarow RM, Isseroff RR, Gomez EC (1992) Quantitative in vitro assessment of phototoxicity by a fibroblast-neutral red assay. J Invest Dermatol 98(5):725–9
18. Wolterbeek HT, van der Meer AJ (2005) Optimization, application, and interpretation of lactate dehydrogenase measurements in microwell determination of cell number and toxicity. Assay Drug Dev Technol 3(6):675–682
19. Vijayalaksmi R, Sathyanarayana MN, Rao MVL (1981) Rubrocurcumin reaction and its use in microdetermination of certain organic acids. Indian J Chem 20B:907
20. Amin A, Gali-Muhtasib H, Ocker M, Schneider-Stock R (2009) Overview of major classes of plant-derived anticancer drugs. Int J Biomed Sci 5:1–11
21. Ji HF, Li XJ, Zhang HY (2009) Can thousands of years of ancient medical knowledge lead us to new and powerful drug combinations in the fight against cancer and dementia EMBO. Nat Prod Rep 10:194–200
22. Huang XH, Jain PK, El Sayed IH, El Sayed MA (2007) Gold nanoparticles: interesting optical properties and recent applications in cancer diagnostic and therapy. Nanomedicine 2:681–693
23. Venu Gopal Y, Ravindranath A, Kalpana G, Rajkapoor B, Sreenivas S (2012) Antitumor and antioxidant activity of *Diospyros peregrina* against Dalton's ascites lymphoma in rodents. Ann Biol Res 3:4985–4992
24. Bose S, Panda AK, Mukherjee S (2015) Curcumin and tumor immune-editing: resurrecting the immune system. Cell Div. https://doi.org/10.1186/s13008-015-0012-z
25. Bernabé Pineda M, Ramírez-Silva MT, Romero-Romo M, González-Vergara E, Rojas-Hernández A (2004) Determination of acidity constants of curcumin in aqueous solution and apparent rate constant of its decomposition. Spectrochim Acta 0(5):1091–1097
26. Souza CRA, Osme SF, Gloria MBA (1997) Stability of curcuminoid pigments in model systems. J Food Process Preserv 21(5):353–363
27. Wang YJ, Pan MH, Cheng AL, Lin LI, Ho YS, Hsieh CY, Lin JK (1997) Stability of curcumin in buffer solutions and characterization of its degradation products. J Pharm Biomed Anal 15(12):1867–1876

28. Germain CS, Niknejad N, Ma L, Garbuio K, Hai T, Dimitroula-kos J (2010) Cisplatin induces cytotoxicity through the mitogen-activated protein kinase pathways and activating transcription factor 3. Neoplasia 12(7): 527–538

29. Kovács AF, Cinatl J (2002) In vitro cytotoxic dose-relation of cisplatin and sodium thiosulphate in human tongue and oesoph-ageal squamous carcinoma cell lines. J Craniomaxillofac Surg 30(1):54–58